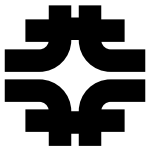

Fermi National Accelerator Laboratory

FERMILAB-Pub-96/187-E
D0

Search for Additional Neutral Gauge Bosons

S. Abachi et al.
The D0 Collaboration

Fermi National Accelerator Laboratory
P.O. Box 500, Batavia, Illinois 60510

July 1996

Submitted to *Physics Letters B*

Operated by Universities Research Association Inc. under Contract No. DE-AC02-76CHO3000 with the United States Department of Energy

Disclaimer

This report was prepared as an account of work sponsored by an agency of the United States Government. Neither the United States Government nor any agency thereof, nor any of their employees, makes any warranty, expressed or implied, or assumes any legal liability or responsibility for the accuracy, completeness, or usefulness of any information, apparatus, product, or process disclosed, or represents that its use would not infringe privately owned rights. Reference herein to any specific commercial product, process, or service by trade name, trademark, manufacturer, or otherwise, does not necessarily constitute or imply its endorsement, recommendation, or favoring by the United States Government or any agency thereof. The views and opinions of authors expressed herein do not necessarily state or reflect those of the United States Government or any agency thereof.

Search for Additional Neutral Gauge Bosons

S. Abachi,[14] B. Abbott,[28] M. Abolins,[25] B.S. Acharya,[43] I. Adam,[12] D.L. Adams,[37] M. Adams,[17] S. Ahn,[14] H. Aihara,[22] J. Alitti,[40] G. Álvarez,[18] G.A. Alves,[10] E. Amidi,[29] N. Amos,[24] E.W. Anderson,[19] S.H. Aronson,[4] R. Astur,[42] R.E. Avery,[31] M.M. Baarmand,[42] A. Baden,[23] V. Balamurali,[32] J. Balderston,[16] B. Baldin,[14] S. Banerjee,[43] J. Bantly,[5] J.F. Bartlett,[14] K. Bazizi,[39] A. Belyaev,[26] J. Bendich,[22] S.B. Beri,[34] I. Bertram,[31] V.A. Bezzubov,[35] P.C. Bhat,[14] V. Bhatnagar,[34] M. Bhattacharjee,[13] A. Bischoff,[9] N. Biswas,[32] G. Blazey,[14] S. Blessing,[15] P. Bloom,[7] A. Boehnlein,[14] N.I. Bojko,[35] F. Borcherding,[14] J. Borders,[39] C. Boswell,[9] A. Brandt,[14] R. Brock,[25] A. Bross,[14] D. Buchholz,[31] V.S. Burtovoi,[35] J.M. Butler,[3] W. Carvalho,[10] D. Casey,[39] H. Castilla-Valdez,[11] D. Chakraborty,[42] S.-M. Chang,[29] S.V. Chekulaev,[35] L.-P. Chen,[22] W. Chen,[42] S. Choi,[41] S. Chopra,[24] B.C. Choudhary,[9] J.H. Christenson,[14] M. Chung,[17] D. Claes,[42] A.R. Clark,[22] W.G. Cobau,[23] J. Cochran,[9] W.E. Cooper,[14] C. Cretsinger,[39] D. Cullen-Vidal,[5] M.A.C. Cummings,[16] D. Cutts,[5] O.I. Dahl,[22] K. De,[44] M. Demarteau,[14] N. Denisenko,[14] D. Denisov,[14] S.P. Denisov,[35] H.T. Diehl,[14] M. Diesburg,[14] G. Di Loreto,[25] R. Dixon,[14] P. Draper,[44] J. Drinkard,[8] Y. Ducros,[40] L.V. Dudko,[26] S.R. Dugad,[43] D. Edmunds,[25] J. Ellison,[9] V.D. Elvira,[42] R. Engelmann,[42] S. Eno,[23] G. Eppley,[37] P. Ermolov,[26] O.V. Eroshin,[35] V.N. Evdokimov,[35] S. Fahey,[25] T. Fahland,[5] M. Fatyga,[4] M.K. Fatyga,[39] J. Featherly,[4] S. Feher,[14] D. Fein,[2] T. Ferbel,[39] G. Finocchiaro,[42] H.E. Fisk,[14] Y. Fisyak,[7] E. Flattum,[25] G.E. Forden,[2] M. Fortner,[30] K.C. Frame,[25] P. Franzini,[12] S. Fuess,[14] E. Gallas,[44] A.N. Galyaev,[35] T.L. Geld,[25] R.J. Genik II,[25] K. Genser,[14] C.E. Gerber,[14] B. Gibbard,[4] V. Glebov,[39] S. Glenn,[7] J.F. Glicenstein,[40] B. Gobbi,[31] M. Goforth,[15] A. Goldschmidt,[22] B. Gómez,[1] G. Gomez,[23] P.I. Goncharov,[35] J.L. González Solís,[11] H. Gordon,[4] L.T. Goss,[45] N. Graf,[4] P.D. Grannis,[42] D.R. Green,[14] J. Green,[30] H. Greenlee,[14] G. Griffin,[8] N. Grossman,[14] P. Grudberg,[22] S. Grünendahl,[39] W.X. Gu,[14,*] G. Guglielmo,[33] J.A. Guida,[2] J.M. Guida,[5] W. Guryn,[4] S.N. Gurzhiev,[35] P. Gutierrez,[33] Y.E. Gutnikov,[35] N.J. Hadley,[23] H. Haggerty,[14] S. Hagopian,[15] V. Hagopian,[15] K.S. Hahn,[39] R.E. Hall,[8] S. Hansen,[14] R. Hatcher,[25] J.M. Hauptman,[19] D. Hedin,[30] A.P. Heinson,[9] U. Heintz,[14] R. Hernández-Montoya,[11] T. Heuring,[15] R. Hirosky,[15] J.D. Hobbs,[14] B. Hoeneisen,[1,†] J.S. Hoftun,[5] F. Hsieh,[24] Tao Hu,[14,*] Ting Hu,[42] Tong Hu,[18] T. Huehn,[9] S. Igarashi,[14] A.S. Ito,[14] E. James,[2] J. Jaques,[32] S.A. Jerger,[25] J.Z.-Y. Jiang,[42] T. Joffe-Minor,[31] H. Johari,[29] K. Johns,[2] M. Johnson,[14] H. Johnstad,[29] A. Jonckheere,[14] M. Jones,[16] H. Jöstlein,[14] S.Y. Jun,[31] C.K. Jung,[42] S. Kahn,[4] G. Kalbfleisch,[33] J.S. Kang,[20] R. Kehoe,[32] M.L. Kelly,[32] L. Kerth,[22] C.L. Kim,[20] S.K. Kim,[41] A. Klatchko,[15] B. Klima,[14] B.I. Klochkov,[35] C. Klopfenstein,[7] V.I. Klyukhin,[35] V.I. Kochetkov,[35] J.M. Kohli,[34] D. Koltick,[36] A.V. Kostritskiy,[35] J. Kotcher,[4] J. Kourlas,[28] A.V. Kozelov,[35] E.A. Kozlovski,[35] J. Krane,[27] M.R. Krishnaswamy,[43] S. Krzywdzinski,[14] S. Kunori,[23] S. Lami,[42] G. Landsberg,[14] B. Lauer,[19] J-F. Lebrat,[40] A. Leflat,[26] H. Li,[42] J. Li,[44] Y.K. Li,[31] Q.Z. Li-Demarteau,[14] J.G.R. Lima,[38] D. Lincoln,[24] S.L. Linn,[15] J. Linnemann,[25] R. Lipton,[14] Y.C. Liu,[31] F. Lobkowicz,[39] S.C. Loken,[22] S. Lökös,[42] L. Lueking,[14] A.L. Lyon,[23] A.K.A. Maciel,[10] R.J. Madaras,[22] R. Madden,[15] L. Magaña-Mendoza,[11] S. Mani,[7] H.S. Mao,[14,*] R. Markeloff,[30] L. Markosky,[2] T. Marshall,[18] M.I. Martin,[14] B. May,[31] A.A. Mayorov,[35] R. McCarthy,[42] T. McKibben,[17]

J. McKinley,[25] T. McMahon,[33] H.L. Melanson,[14] J.R.T. de Mello Neto,[38] K.W. Merritt,[14] H. Miettinen,[37] A. Mincer,[28] J.M. de Miranda,[10] C.S. Mishra,[14] N. Mokhov,[14] N.K. Mondal,[43] H.E. Montgomery,[14] P. Mooney,[1] H. da Motta,[10] M. Mudan,[28] C. Murphy,[17] F. Nang,[5] M. Narain,[14] V.S. Narasimham,[43] A. Narayanan,[2] H.A. Neal,[24] J.P. Negret,[1] E. Neis,[24] P. Nemethy,[28] D. Nešić,[5] M. Nicola,[10] D. Norman,[45] L. Oesch,[24] V. Oguri,[38] E. Oltman,[22] N. Oshima,[14] D. Owen,[25] P. Padley,[37] M. Pang,[19] A. Para,[14] C.H. Park,[14] Y.M. Park,[21] R. Partridge,[5] N. Parua,[43] M. Paterno,[39] J. Perkins,[44] A. Peryshkin,[14] M. Peters,[16] H. Piekarz,[15] Y. Pischalnikov,[36] V.M. Podstavkov,[35] B.G. Pope,[25] H.B. Prosper,[15] S. Protopopescu,[4] D. Pušeljić,[22] J. Qian,[24] P.Z. Quintas,[14] R. Raja,[14] S. Rajagopalan,[42] O. Ramirez,[17] M.V.S. Rao,[43] P.A. Rapidis,[14] L. Rasmussen,[42] S. Reucroft,[29] M. Rijssenbeek,[42] T. Rockwell,[25] N.A. Roe,[22] P. Rubinov,[31] R. Ruchti,[32] J. Rutherfoord,[2] A. Sánchez-Hernández,[11] A. Santoro,[10] L. Sawyer,[44] R.D. Schamberger,[42] H. Schellman,[31] J. Sculli,[28] E. Shabalina,[26] C. Shaffer,[15] H.C. Shankar,[43] R.K. Shivpuri,[13] M. Shupe,[2] J.B. Singh,[34] V. Sirotenko,[30] W. Smart,[14] A. Smith,[2] R.P. Smith,[14] R. Snihur,[31] G.R. Snow,[27] J. Snow,[33] S. Snyder,[4] J. Solomon,[17] P.M. Sood,[34] M. Sosebee,[44] N. Sotnikova,[26] M. Souza,[10] A.L. Spadafora,[22] R.W. Stephens,[44] M.L. Stevenson,[22] D. Stewart,[24] D.A. Stoianova,[35] D. Stoker,[8] K. Streets,[28] M. Strovink,[22] A. Sznajder,[10] P. Tamburello,[23] J. Tarazi,[8] M. Tartaglia,[14] T.L. Taylor,[31] J. Thompson,[23] T.G. Trippe,[22] P.M. Tuts,[12] N. Varelas,[25] E.W. Varnes,[22] P.R.G. Virador,[22] D. Vititoe,[2] A.A. Volkov,[35] A.P. Vorobiev,[35] H.D. Wahl,[15] G. Wang,[15] J. Warchol,[32] G. Watts,[5] M. Wayne,[32] H. Weerts,[25] A. White,[44] J.T. White,[45] J.A. Wightman,[19] J. Wilcox,[29] S. Willis,[30] S.J. Wimpenny,[9] J.V.D. Wirjawan,[45] J. Womersley,[14] E. Won,[39] D.R. Wood,[29] H. Xu,[5] R. Yamada,[14] P. Yamin,[4] C. Yanagisawa,[42] J. Yang,[28] T. Yasuda,[29] P. Yepes,[37] C. Yoshikawa,[16] S. Youssef,[15] J. Yu,[14] Y. Yu,[41] Q. Zhu,[28] Z.H. Zhu,[39] D. Zieminska,[18] A. Zieminski,[18] E.G. Zverev,[26] and A. Zylberstejn[40]

(DØ Collaboration)

[1] *Universidad de los Andes, Bogotá, Colombia*
[2] *University of Arizona, Tucson, Arizona 85721*
[3] *Boston University, Boston, Massachusetts 02215*
[4] *Brookhaven National Laboratory, Upton, New York 11973*
[5] *Brown University, Providence, Rhode Island 02912*
[6] *Universidad de Buenos Aires, Buenos Aires, Argentina*
[7] *University of California, Davis, California 95616*
[8] *University of California, Irvine, California 92717*
[9] *University of California, Riverside, California 92521*
[10] *LAFEX, Centro Brasileiro de Pesquisas Físicas, Rio de Janeiro, Brazil*
[11] *CINVESTAV, Mexico City, Mexico*
[12] *Columbia University, New York, New York 10027*
[13] *Delhi University, Delhi, India 110007*
[14] *Fermi National Accelerator Laboratory, Batavia, Illinois 60510*
[15] *Florida State University, Tallahassee, Florida 32306*
[16] *University of Hawaii, Honolulu, Hawaii 96822*
[17] *University of Illinois at Chicago, Chicago, Illinois 60607*

[18] *Indiana University, Bloomington, Indiana 47405*
[19] *Iowa State University, Ames, Iowa 50011*
[20] *Korea University, Seoul, Korea*
[21] *Kyungsung University, Pusan, Korea*
[22] *Lawrence Berkeley National Laboratory and University of California, Berkeley, California 94720*
[23] *University of Maryland, College Park, Maryland 20742*
[24] *University of Michigan, Ann Arbor, Michigan 48109*
[25] *Michigan State University, East Lansing, Michigan 48824*
[26] *Moscow State University, Moscow, Russia*
[27] *University of Nebraska, Lincoln, Nebraska 68588*
[28] *New York University, New York, New York 10003*
[29] *Northeastern University, Boston, Massachusetts 02115*
[30] *Northern Illinois University, DeKalb, Illinois 60115*
[31] *Northwestern University, Evanston, Illinois 60208*
[32] *University of Notre Dame, Notre Dame, Indiana 46556*
[33] *University of Oklahoma, Norman, Oklahoma 73019*
[34] *University of Panjab, Chandigarh 16-00-14, India*
[35] *Institute for High Energy Physics, 142-284 Protvino, Russia*
[36] *Purdue University, West Lafayette, Indiana 47907*
[37] *Rice University, Houston, Texas 77005*
[38] *Universidade Estadual do Rio de Janeiro, Brazil*
[39] *University of Rochester, Rochester, New York 14627*
[40] *CEA, DAPNIA/Service de Physique des Particules, CE-SACLAY, France*
[41] *Seoul National University, Seoul, Korea*
[42] *State University of New York, Stony Brook, New York 11794*
[43] *Tata Institute of Fundamental Research, Colaba, Bombay 400005, India*
[44] *University of Texas, Arlington, Texas 76019*
[45] *Texas A&M University, College Station, Texas 77843*
(submitted June 28, 1996)

Abstract

We have searched for a heavy neutral gauge boson, Z', using the decay channel $Z' \to ee$. The data were collected with the DØ detector at the Fermilab Tevatron during the 1992–1993 $p\overline{p}$ collider run at $\sqrt{s} = 1.8$ TeV from an integrated luminosity of 15 ± 1 pb^{-1}. Limits are set on the cross section times branching ratio for the process $p\overline{p} \to Z' \to ee$ as a function of the Z' mass. We exclude the existence of a Z' of mass less than 490 GeV/c^2, assuming a Z' with the same coupling strengths to quarks and leptons as the standard model Z boson.

PACS numbers: 13.85.Rm, 12.60.Cn, 14.70.Hp.
Keywords: Experimental; Limits; New gauge bosons; Z'.

I. INTRODUCTION

Additional heavy neutral gauge bosons, generically called Z', and heavy charged gauge bosons, W', are predicted by numerous extensions to the standard model. One of the earliest of these extensions is the left-right model, the addition of a right-handed gauge group to the electroweak sector giving $SU(2)_R \times SU(2)_L \times U(1)$ [1]. A left-right model embedded in a supersymmetric $SO(10)$ group generates W' and Z', possibly detectable at present colliders [2]. E_6 is the next natural symmetry group for a unified theory beyond $SO(10)$. It generated much theoretical interest because it was the simplest unifying group inspired by superstring theory [3]. In one version, E_6 decomposes into a form of $SU(2)_R \times SU(2)_L \times U(1)$ called the alternative left-right model that also predicts a W' and Z' that could be detected at present colliders [4]. There are many superstring-derived unified models that contain additional $U(1)$ symmetry groups, possibly leading to detectable additional neutral gauge bosons [5].

Reported searches for Z' typically set a limit on the Z' mass based on a particular model. A reference model Z' with the same coupling strengths to quarks and leptons as the standard model Z boson and with decay to W and Z bosons suppressed is traditionally used for this purpose. There is no theoretical prediction for a Z' of this type but it is a useful standard reference [6]. Except where noted, all mass limits in this paper refer to a Z' of this type. Many specific Z' models are expected to have smaller cross sections than this model, so the mass limit for a specific Z' can be substantially less [7].

Indirect limits on Z' production coming from weak neutral current experiments, precision measurement at the Z pole, and the W mass measurement are combined with a direct collider limit to exclude Z' with mass less than 750 GeV/c^2 at the 95% confidence level (CL), but, for a specific E_6 model Z', the limit can be as low as 160 GeV/c^2 [6]. Previous direct searches in $p\overline{p}$ collisions have set a limit $m_{Z'} > 505$ GeV/c^2 (95% CL) [8]. Previous direct searches for W' have set a limit $m_{W'} > 720$ GeV/c^2 (95% CL) [9]. This result restricts Z' from a left-right model to $m_{Z'} > m_{W'} > 720$ GeV/c^2 (95% CL), depending on theoretical assumptions [2]. In this paper, we present the results of a search using the DØ detector [10] for a heavy ($m_{Z'} > m_Z$) neutral gauge boson decaying through the channel $Z' \to ee$.

II. EXPERIMENTAL METHOD

The data were collected at the Fermilab Tevatron during the 1992–1993 $p\overline{p}$ collider run at $\sqrt{s} = 1.8$ TeV from an integrated luminosity of 15 ± 1 pb^{-1}. We search for the Breit-Wigner peak of a Z' superimposed on the invariant mass spectrum expected in the standard model from Z continuum and Drell-Yan production Z, γ^* decaying to electron-positron pairs ee. We set a limit on the cross section times branching ratio σB for the process $p\overline{p} \to Z' \to ee$ and use this limit to set a lower bound on the mass of a reference model Z'.

The DØ detector consists of a central tracking system, a calorimeter, and a muon spectrometer. The central tracking system detects tracks from charged particles within the pseudorapidity range $|\eta| < 3$ [11]. The calorimeter is hermetic with coverage to $|\eta| = 4$. It employs depleted uranium absorber and liquid argon ionization layers. The electromagnetic (EM) section consists of the four innermost concentric layers with segmentation 0.1×0.1 ($\Delta\eta \times \Delta\phi$) in layers 1, 2, and 4 and 0.05×0.05 in layer 3 at shower maximum. It is 21

radiation lengths in depth. The calorimeter is in three units, a central barrel (CC) and two end caps (EC).

III. EVENT SELECTION

The trigger for the data sample requires two isolated EM clusters with transverse energy $E_T > 20$ GeV [12] and shape consistent with that of an electron, which come from two 0.2×0.2 ($\Delta\eta \times \Delta\phi$) EM trigger towers with energy $E > 7$ GeV. Candidate events are reconstructed off-line and the electron energy is corrected by using the Z boson mass for calibration. To be included in the final sample, candidate events are required to have two electrons with $E_T > 30$ GeV. This value is chosen to be safely above the trigger threshold but to retain substantial Z signal and be nearly fully efficient for Z' with mass above the current limit. The fiducial region for electrons in the CC is $|\eta| < 1.1$, and $1.5 < |\eta| < 2.5$ in the EC. In the CC, energy clusters located within 0.01 radians in ϕ of module boundaries located every 0.2 radians in ϕ are excluded.

The principal background to Z, Drell-Yan, and possible Z' in the data is QCD multijet events in which jets are reconstructed as electrons. Fake electrons can arise from jets in which a neutral pion carrying most of the jet energy overlaps with a charged particle, from the charge exchange interaction of charged pions near the front surface of the EM calorimeter, and from converted photons, principally from neutral pion decay. In addition, heavy quark decays can produce real electrons. The following selection criteria are imposed on the EM energy clusters to reduce the background from fake electrons and real electrons within jets. A more detailed description is available in Ref. [13].

The electron energy is determined by a clustering algorithm using energy deposited in the EM section and the first hadronic layer of the calorimeter. The EM fraction is defined as $E^{EM}/(E + E^{\rm other})$, where E is the electron energy, E^{EM} is the electron energy in the EM layers of the calorimeter, and $E^{\rm other}$ is associated energy from the hadronic layers of the calorimeter not included in the electron clustering algorithm. The requirement is EM fraction > 0.9.

Isolation is defined as $(E_{T,R=0.4} - E^{EM}_{T,R=0.2})/E^{EM}_{T,R=0.2}$, where $E_{T,R=0.4}$ is the transverse energy in the calorimeter within a cone of radius $R = 0.4$ in η, ϕ space from the energy weighted center of the cluster. $E^{EM}_{T,R=0.2}$ is the transverse energy in the EM layers of the calorimeter. The requirement is isolation < 0.15.

A covariance matrix of 41 parameters describing the electromagnetic shower shape as a function of position in the calorimeter is determined from simulated electron showers. The covariance matrix may be diagonalized with a unitary transformation. In this basis, the parameter χ^2 is defined as $\chi^2 = \sum_{i=1}^{41}(y'_i - \overline{y}_i)^2/\sigma_i^2$ where y'_i are uncorrelated variables in the data describing an electromagnetic shower and $\overline{y}_i$ and σ_i^2 are the mean and variance determined by the simulation. The requirement is $\chi^2 < 200$.

We further require that at least one of the energy clusters have a matching track in the central tracking system with significance $S < 5$. Track match significance is defined in the CC as $S = ((\Delta z/\delta\Delta z)^2 + (\Delta\phi/\delta\Delta\phi)^2)^{1/2}$, where for each variable Δx is the mismatch between the track and the energy weighted center of the cluster and $\delta\Delta x$ is the resolution of that variable. For the EC, substitute Δr for Δz, where r is the cylindrical coordinate.

Additionally, at least one of the electrons must be in the CC. For $m_{ee} > 150$ GeV/c^2, almost all rejected events would have one electron in each of the end cap calorimeters. For this forward-backward topology, the estimated QCD background exceeds the expected Z' signal. For $m_{Z'} = 500$ GeV/c^2, the topological cut reduces the acceptance for Z' by $\approx 7\%$.

The total acceptance for the Z boson, including all selection efficiencies, is 25%. For a 500 GeV/c^2 Z', the total acceptance is 43%.

IV. BACKGROUND

There are 886 events selected using the above criteria. The QCD multijet background remaining in this data sample is determined from data. An event sample is selected by requiring one apparent electron which passes the preceding electron identification requirements and one jet which satisfies the kinematic and fiducial requirements for electrons. The contribution of real electrons from W and Z boson decays in this sample is small. The cross section for apparent electrons in dijet events obtained from this sample is divided by the exclusive dijet cross section for jets with $E_T > 30$ GeV to get the rate for apparent electrons per jet, e/j. The rate per jet for apparent electrons with a matching track is $0.4\ (0.9) \times 10^{-3}$ in the CC (EC) and $1.8\ (2.5) \times 10^{-3}$ without a track requirement. The predicted number of QCD multijet events in the data sample can be calculated from the rate e/j and the inclusive dijet cross section, assuming that the probability of a given jet being identified as an electron is uncorrelated within a multijet event. Making appropriate allowances for the different rates in the CC and EC and for electrons with and without a matching track requirement, the predicted background is 38 ± 3 events. Physics background processes in the data sample, including $Z \rightarrow \tau\tau \rightarrow ee$, are negligible.

V. MONTE CARLO

Physics processes are simulated using the PYTHIA Monte Carlo (version 5.7) [14], with MRS D$-'$ parton distribution functions (pdf's) [15]. The pdf sets MRS D0$'$ and CTEQ 2M [16] are used to evaluate the uncertainty due to the choice of pdf's. The principal physics background to Z' production is Z and Drell-Yan production, $q\overline{q} \rightarrow Z \rightarrow ee$ and $q\overline{q} \rightarrow \gamma^* \rightarrow ee$. The interference between these two processes is included in the Monte Carlo. The Monte Carlo output is smeared for detector energy and angular resolution. The energy resolution is given by

$$\frac{\sigma_E}{E} = \alpha \oplus \frac{\beta}{\sqrt{E_s(\mathrm{GeV})}} \oplus \frac{\delta}{E(\mathrm{GeV})},$$

where E_s is E_T for CC and E for EC. The energy and angular resolution used are shown in Table I. To model the detector acceptance realistically, the z position of the event vertex is generated using a Gaussian shape centered at 8.5 cm with a standard deviation of 27 cm, reflecting the distribution seen in the data.

Trigger and electron identification efficiencies are different for the CC and EC. This difference is introduced into the Monte Carlo by giving different weights to events with both

electrons in the CC and events with one central electron and one in the EC. The weights are chosen to reproduce the proportion of these two types of events observed in the data after QCD background is subtracted. The smeared Z and Drell-Yan invariant mass spectrum and the QCD dijet invariant mass spectrum are shown in Fig. 1. The number of simulated events is normalized to the number of observed events after QCD background is subtracted. The dielectron invariant mass spectrum from data is compared to the sum of Z and Drell-Yan Monte Carlo plus QCD background spectra in Fig. 2. The agreement is good. In the absence of Z', for $m_{ee} > 170$ GeV/c^2 we expect 8.2 ± 0.4 Z and Drell-Yan plus QCD background events. Twelve events are observed in the data.

A combined Z', Z, and Drell-Yan signal is also modeled by Monte Carlo. Z' is produced by $q\overline{q} \rightarrow Z' \rightarrow ee$ so it interferes with Z,$\gamma*$. Because of the interference effects, it is not possible to generate a Z' signal independently. The difference between the Z', Z, γ^* and Z, γ^* Monte Carlo signals is the Z' signal. Z' signals are generated for $m_{Z'} = 100$ to 600 GeV/c^2 in order to set a limit on Z' production over this range.

The Z' width , $_{Z'}$ is assumed to scale with the Z' mass, , $_{Z'} = (m_{Z'}/m_Z)$, $_Z$. This scaling is what would be expected for a reference model Z'. For $m_{Z'} \geq 400$ GeV/c^2, the decay channel to top quarks is assumed to be open. Choosing this scaling is a conservative assumption since in E_6 and left-right symmetric models, the Z' width would be substantially narrower than this [17]. The width of a Z' from a superstring model is, in general, expected to be less than 2.5% of the Z' mass [18].

The kinematic and fiducial acceptance for the Z' is taken from the Monte Carlo. The trigger and reconstruction efficiencies within the acceptance are assumed to be the same for Z' as for the Z. This is substantiated by data from test beam electrons up to 150 GeV and by simulation of high energy electrons. There is a 3% uncertainty in the ratio of the kinematic and geometric acceptance for the Z' to that of the Z which arises from the choice of parton distribution functions, radiative corrections, and statistical precision in the Monte Carlo.

VI. LIMITS

A binned likelihood approach with Poisson statistics is applied to the invariant mass distribution to obtain an upper limit on the process $p\overline{p} \rightarrow Z' \rightarrow ee$. The procedure is the same as that in Ref. [19]. The probability density function for the Z' is constructed using the invariant mass region where substantial Z' signal is expected. The lower bound of the invariant mass region is given in Table II. The binning is chosen so that the number of expected Z' events is approximately equal in each bin. Ten bins are used. The limit on expected Z' events, $N_{95}^{Z'}$, is expressed as a 95% CL limit on $\sigma B(Z' \rightarrow ee)/\sigma B(Z \rightarrow ee)$ using

$$\left(\frac{(\sigma B)_{Z' \rightarrow ee}}{(\sigma B)_{Z \rightarrow ee}}\right)_{95} = \frac{A_Z}{A_{Z'} N_Z} N_{95}^{Z'}.$$

The acceptance for Z', $A_{Z'}$, is given by

$$A_{Z'} = \frac{(\sigma BA)_{Z',Z,\gamma^* \rightarrow ee} - (\sigma BA)_{Z,\gamma^* \rightarrow ee}}{(\sigma B)_{Z' \rightarrow ee}},$$

where the acceptances are for the invariant mass region included in the probability density function. A_Z/N_Z is given by

$$\frac{A_Z}{N_Z} = \frac{(\sigma BA)_{Z,\gamma^* \to ee}}{(\sigma B)_{Z \to ee} N_{Z,\gamma^*}},$$

where N_{Z,γ^*} is equal to the number of observed events after QCD background is subtracted. The acceptances in this case are for the full invariant mass spectrum. The uncertainty in $A_Z/(A_{Z'}N_Z)$ is incorporated in the probability distribution. This uncertainty consists of the 3% uncertainty in $A_{Z'}/A_Z$ and the 4% uncertainty in $N_{Z,\gamma*}$.

The 95% CL limit on the ratio $\sigma B(Z' \to ee)/\sigma B(Z \to ee)$ plotted as a function of the Z' mass together with the value of this ratio for a reference model Z' are shown in Fig. 3. Table II gives the 95% CL limit on this ratio, the limit expressed as expected Z' events, and the observed events for the different Z' masses considered. The theoretical cross section ratio is determined using Born level cross sections [14] and a second order scaling factor, $K2$ [20]. $K2$ is applied to the Born level cross section as a function of the 4-momentum transfer q^2. There is a 3% uncertainty in the theory due to the choice of pdf's. This uncertainty is not incorporated into the 95% CL limit curve since that limit is independent of the cross section for any specific Z' model. The effect of this error on the mass limit would, in any event, be negligible.

VII. CONCLUSIONS

We have searched for an additional neutral gauge boson from the process $p\overline{p} \to Z' \to ee$. This process is excluded at the 95% CL for the area above the limit curve in Fig. 3. From the intersection of the limit curve and the theory curve, we exclude the existence of a Z' boson with the same coupling strengths to quarks and leptons as the standard model Z boson for $m_{Z'} < 490$ GeV/c^2 (95% CL).

ACKNOWLEDGEMENTS

We thank the staffs at Fermilab and the collaborating institutions for their contributions to the success of this work, and acknowledge support from the Department of Energy and National Science Foundation (U.S.A.), Commissariat à L'Energie Atomique (France), Ministries for Atomic Energy and Science and Technology Policy (Russia), CNPq (Brazil), Departments of Atomic Energy and Science and Education (India), Colciencias (Colombia), CONACyT (Mexico), Ministry of Education and KOSEF (Korea), CONICET and UBACyT (Argentina), and the A.P. Sloan Foundation.

REFERENCES

* Visitor from IHEP, Beijing, China.
† Visitor from Univ. San Francisco de Quito, Ecuador.

[1] For a general survey and original references see R.N. Mohapatra, *Unification and Supersymmetry*, Springer-Verlag, New York, 1992.
[2] T.G. Rizzo, Phys. Rev. D **50**, 325 (1994).
[3] J.L. Hewett and T.G. Rizzo, Phys. Rep. **183**, 193 (1989).
[4] E. Ma, Phys. Rev. D **36**, 274 (1987); K. Babu, X. He, and E. Ma, Phys. Rev. D **36**, 878 (1987).
[5] M. Cvetič and P. Langacker, U. of Pennsylvania Report, UPR-0690-T (1996).
[6] P. Langacker and M. Luo, Phys. Rev. D **45**, 278 (1991).
[7] J.L. Hewett and T.G. Rizzo, U. of Wisconsin Report, MAD-PH-645 (1991).
[8] CDF Collaboration, F. Abe *et al.*, Phys. Rev. D **51**, 949 (1995).
[9] DØ Collaboration, S. Abachi *et al.*, Phys. Rev. Lett. **76**, 3271 (1996).
[10] DØ Collaboration, S. Abachi *et al.*, Nucl. Instrum. Methods A **338**, 185 (1994).
[11] The DØ detector is described in cylindrical coordinates r, ϕ, and z with the z axis coincident with the beam and $z = 0$ at the nominal center of the interaction area. The spherical coordinates θ and ϕ are also used. Pseudorapidity is defined as $\eta \equiv \tanh^{-1}(\cos\theta)$.
[12] Transverse energy E_T is the projection of the energy, taken as a vector, in the plane orthogonal to the beam direction.
[13] DØ Collaboration, S. Abachi *et al.*, Phys. Rev. D **52**, 4877 (1995).
[14] T. Sjöstrand, Computer Physics Commun. **82**, 74 (1994).
[15] A.D. Martin, R.G. Roberts and W.J. Stirling, Phys. Lett. B **306**, 145 (1993); *Erratum* Phys. Lett. B **309**, 492 (1993).
[16] CTEQ Collaboration, J. Botts *et al.*, Phys. Lett. B **304**, 159 (1993).
[17] G. Eppley and H.E. Miettinen, SDC Collaboration Note, SDC-90-00125 (1990).
[18] J.L. Rosner, Phys. Rev. D **35**, 2244 (1987).
[19] DØ Collaboration, S. Abachi *et al.*, Phys. Lett. B **358**, 405 (1995).
[20] R. Hamberg, W.L. van Neerven, and T. Matsuura, Nucl. Phys. B **359**, 343 (1991).

FIGURES

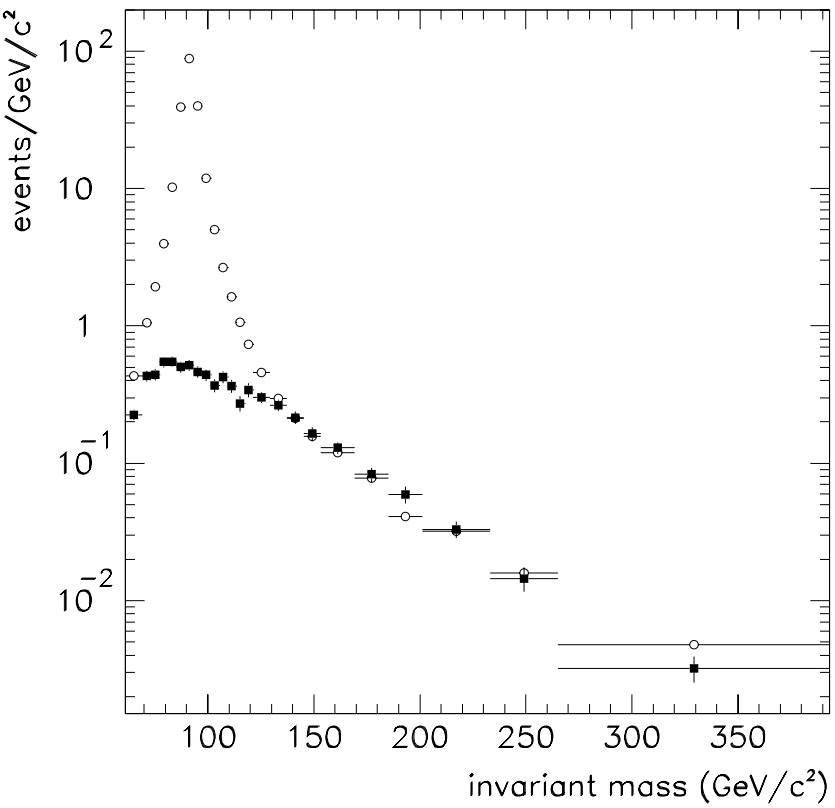

FIG. 1. The expected backgrounds to Z': Z and Drell-Yan (open circles) and QCD multijet (solid squares).

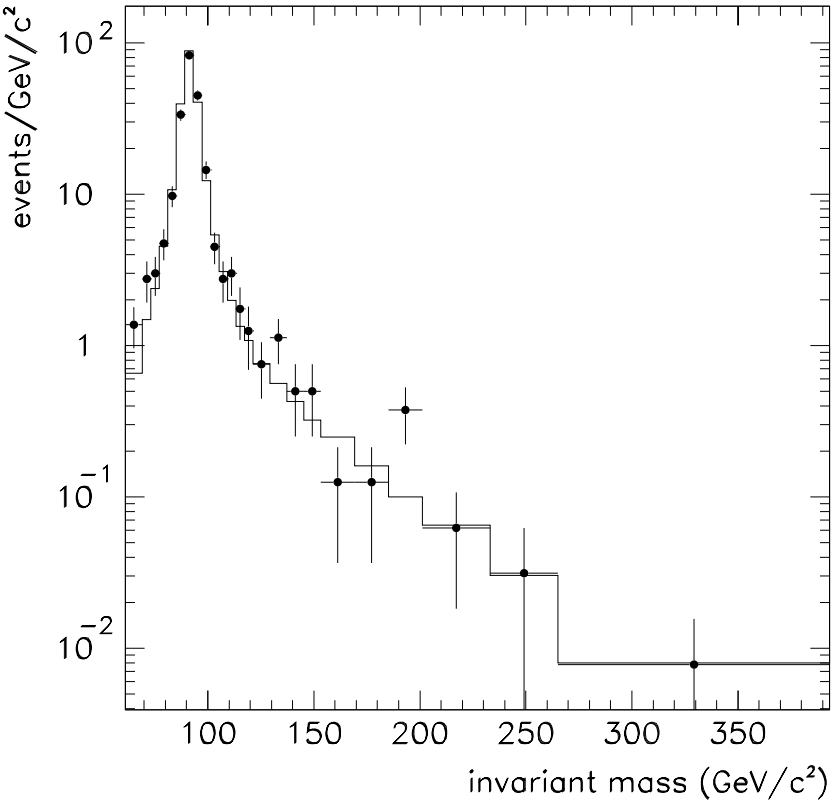

FIG. 2. Observed dielectron events (discrete points) are compared to the combined Z, Drell-Yan, and QCD background.

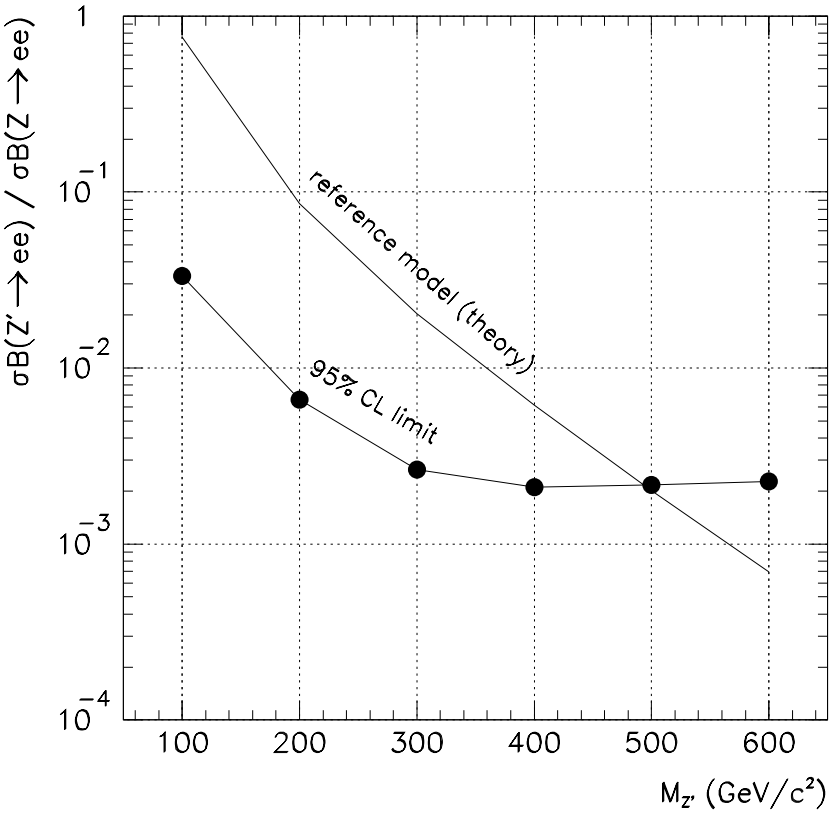

FIG. 3. 95% CL upper limit as a function of $m_{Z'}$ for $\sigma B(Z' \to ee)/\sigma B(Z \to ee)$. The expected theoretical value using standard model Z couplings is also shown.

TABLES

	Constant α (%)	Sampling β (%$\sqrt{\text{GeV}}$)	Noise δ (GeV)	$\delta\theta$ (radians)	$\delta\phi$ (radians)
CC	1.0	13.0	0.4	0.058	0.014
EC	0.3	16.0	0.4	0.027	0.031

TABLE I. Parameters used to smear the Monte Carlo for energy resolution and angular resolution for electrons.

$m_{Z'}$ (GeV/c^2)	m_{ee} min., binning	observed events	95% CL, $N_{95}^{Z'}$	95% CL, $\sigma B_{Z'}/\sigma B_Z$ ($\times 10^{-3}$)
100	95	226	30.09	33.32
200	170	12	9.38	6.61
300	255	1	3.86	2.65
400	340	0	3.02	2.11
500	425	0	3.02	2.17
600	510	0	3.02	2.26

TABLE II. For each Z' mass: minimum m_{ee} of the fit region, the number of observed events, the 95% CL expressed as expected Z' events, and the 95% CL expressed as $\sigma B(Z' \to ee)/\sigma B(Z \to ee)$.